

## Effect of time reversal symmetry on states of quasi – particles in crystals

**H W Kunert**

Department of Physics, University of Pretoria, 0001 Pretoria, South Africa.

Email: hkunert@nsnper1.up.ac.za

**Abstract.** The problem of additional time reversal (*TR*) degeneracy and the transformation properties of “time reversed” wave functions are investigated. In crystals the one electron Hamiltonian is invariant with respect to a space group of a crystal. The Bloch functions are the basis for irreducible representations (irrp’s) of the wave vector groups  $\mathbf{k}$ . When an irrp is complex the *TR* symmetry must be considered. Using Herring’s criterion adopted to space groups we have investigated several hexagonal materials for optoelectronic devices such as ZnO, GaN, 6H-SiC. We have found many complex irrps. We discuss the effect of the *TR* on vibrational and electronic states together with optical selection rules in ZnO and GaN. In addition we list all complex irrps of the 32 crystallographic double point groups. Spin is taken into account throughout the whole discussion.

### 1. Introduction

States of quasiparticles in crystals such as electrons in conduction bands, holes in valence bands, excitons, phonons, plasmons, polaritons, etc., in short: “ons”, are classified according to irrps of factor wave vector groups  $G^{\mathbf{k}}/T$ . Here the vector  $\mathbf{k}$  runs over the entire first BZ and denotes three quantum numbers  $k_x$ ,  $k_y$  and  $k_z$ . For hexagonal BZ the factor groups are determined by high symmetry points  $\Gamma = GM, A, M, K, L, H$ , and lines  $R, Q, S, \Delta = LD, \Sigma = SM, \Lambda = LD, T, U$ , and  $P$ . The generators of irrps and the characters of the corresponding factor groups  $G^{\mathbf{k}\Gamma}/T, \dots, G^{\mathbf{k}U}/T$ , have been tabulated (CDML [1]). When an irrp  $D$  is complex, an extra *TR* degeneracy may occur. In such case any state of “ons” will be classified according the “joint” reps  $D \oplus D^*$ . This will affect many phenomena. For example, it will increase the dimension of the dynamical matrices. It will change the selection rules for optical transitions. It will also influence the scattering tensors and many other physical processes taking place in a crystal. It is therefore of importance to find out which irrps of a crystal are complex before analysis of experimental data.

In this contribution we use Herring [2,3] criterion for investigation of complex irrps modified by inclusion of spin and effect of *TR* operator on behaviour of wave vectors of a star  $\{\mathbf{k}^*\}$  of the factor space group  $C_{6v}^4 - P6_3/mc$  for ZnO, GaN, 6H-SiC, BeO, CdS, ZnS and many others.

The scope of the paper is following: In section 2 we discuss some theoretical aspects of the *TR* operator and Herring’s criterion. In section 3 we analyze the experimental dispersion curves obtained by neutron scattering technique [4,5]. In section 3 we give some examples for complex irrps calculation. The section 4 is devoted to vibrational modes in wurtzite crystals due to *TR* symmetry. In section 5 we discuss the electronic band structure and optical selection rules in presence of *TR*. Complex irrps of 32 double crystallographic point groups and of  $C_{6v}^4$  space group are listed explicitly.

## 2. Theoretical background

### 2.1. Time reversal operator for spinless particles. $T = K$

Consider a quantum mechanical system described by the time-dependent Schroedinger equation

$$\frac{ih}{2\pi} \frac{\partial \Psi(\mathbf{r}, t)}{\partial t} = \left\{ \left( \frac{-h}{2\pi} \right)^2 \frac{1}{2m} \nabla^2 + V(\mathbf{r}) \right\} \Psi(\mathbf{r}, t) \quad (1)$$

Replacing  $t$  by  $-t$  and taking the complex conjugate of both sides of the above equation, we have

$$\frac{ih}{2\pi} \frac{\partial \Psi^*(\mathbf{r}, -t)}{\partial t} = \left\{ \left( \frac{-h}{2\pi} \right)^2 \frac{1}{2m} \nabla^2 + V(\mathbf{r}) \right\} \Psi^*(\mathbf{r}, -t) \quad (2)$$

This shows that  $\Psi^*(\mathbf{r}, -t)$  is also a solution of Schroedinger equation if  $\Psi(\mathbf{r}, t)$  is.

Clearly, for spinless particles the  $K$  has the effect of reversing the direction of propagation of time and it is just the complex conjugation operator apart from a phase factor, usually denoted as  $\exp\{-iEt/(h/2\pi)\}$ . The matrices for  $\mathbf{r}$  and  $\mathbf{p}$  are real and purely imaginary so that the complex conjugation operator  $K$  has the following effect on  $\mathbf{r}$  and  $\mathbf{p}$ , and the operation of  $T$  on a wave function gives its complex conjugate:

$$K\mathbf{r}K^+ = \mathbf{r} \quad (3a)$$

$$K\mathbf{p}K^+ = -\mathbf{p} \quad (3b)$$

$$T\Psi(\mathbf{r}) = \Psi^*(\mathbf{r}) \quad (3c)$$

$$T = K \quad (3d)$$

In the equation (3d) we have chosen the phase factor to be unity.

### 2.2. Time reversal operator for spin $-1/2$ particles, $s_y = 1/2(h/2\pi)\sigma_y$ . $T = -i\sigma_y K$

In order to define the  $TR$  operator for particles with spin we follow the transformation properties of dynamical variables  $\mathbf{r}$ ,  $\mathbf{p}$ ,  $\mathbf{s}$  and  $\mathbf{j}$  [5]. It is clear that

$$T\mathbf{r}T^+ = \mathbf{r} \quad (4a)$$

$$T\mathbf{p}T^+ = -\mathbf{p} \quad (4b)$$

$$T(\mathbf{r} \times \mathbf{p})T^+ = -(\mathbf{r} \times \mathbf{p}) \quad (4c)$$

$$T\mathbf{s}T^+ = -\mathbf{s} \quad (4d)$$

$$T\mathbf{j}T^+ = -\mathbf{j} \quad (4e)$$

$$Ks_xK^+ = s_x \quad (5a)$$

$$Ks_yK^+ = s_y \quad (5b)$$

$$Ks_zK^+ = s_z \quad (5c)$$

$$T = UK \quad (5d)$$

$$K^2 = 1 \quad (5e)$$

$$TK = U \quad (5f)$$

for the particle with spin. The last equation (4) is in the standard  $(\mathbf{r}, s_z)$  representation in which  $s_x$  and  $s_z$  are real whereas the  $s_y$  matrix is imaginary. The  $U$  is to be determined. The  $T$  and  $K$  are antiunitary operators. Using equations (3a, b; 4a, b, d, e; 5a, b, c) we obtain

$$U = \exp[-i\pi s_y / (h/2\pi)] \quad (6a)$$

$$T = \exp[-i\pi s_y / (h/2\pi)]K \quad (6b)$$

$$T = -i\sigma_y K \quad (6c)$$

The equation (6c) represents the time reversal operator  $T$  for a spin  $-1/2$  particle,  $s_y = 1/2(h/2\pi)\sigma_y$ , which follows from theory of the  $SO(2)$  group [6,7]. The equation(6c) can be easily extended to a system of  $n$  particles having arbitrary spin angular momenta. The extension leads to the Kramers' theorem which will not be discussed here.

### 2.3. Criteria for real and complex irreducible representations. Point groups

Frobenius and Shur [8] showed that it is sufficient knowing only the characters of an irrep to determine whether the rep is real or complex. If the sum of characters of squares of the group elements is equal to the order of the group  $|g|$ , then the reps is real: if the sum is  $-|g|$ , the rep is equivalent to its conjugate: and if the sum vanishes the reps  $D$  and  $D^*$  are complex and inequivalent. For single and double valued (spin included) irreps of 32 crystallographic point groups we write

$$1, \text{ case (a) } D \text{ is real} \quad (7a)$$

$$(1/|g|) \sum_{g \in G} \chi(g^2) = 0, \text{ case (b) } D \text{ and } D^* \text{ are complex and inequivalent} \quad (7b)$$

$$-1, \text{ case (c) } D \text{ and } D^* \text{ are complex and equivalent} \quad (7c)$$

In terms of basis functions  $\Psi$  of  $D$  and  $\Psi^*$  of  $D^*$  for case (a) the functions  $\Psi$  and  $\Psi^*$  are linearly dependent and no extra degeneracy occurs, for cases (b) and (c)  $\Psi$  and  $\Psi^*$  are linearly independent and an extra degeneracy occurs. Using the criteria we have tested all single and double valued (spin included – spinor) irreps of the 32 point group. The results are listed in table 1.

### 2.4. Criteria for real and complex irreducible representations. Space groups

The basis of irreps of space groups are Bloch functions  $\Psi_{\mathbf{k}}(\mathbf{r}) = u(\mathbf{r})\exp(i\mathbf{k}\mathbf{t})$ , where the  $\mathbf{k}$  runs over the entire first BZ and  $\mathbf{t}$  are translations. As stated in Chapter 2, when spin excluded, the  $TR$  operator is just complex conjugation action on function. That means:  $T\Psi_{\mathbf{k}}(\mathbf{r}) = T\{u(\mathbf{r})\exp(i\mathbf{k}\mathbf{t})\} = u^*(\mathbf{r})\exp[i(-\mathbf{k})\mathbf{t}]$ . Clearly, the  $TR$  operator transforms vector  $\mathbf{k}$  into  $-\mathbf{k}$ . That is an important effect which leads us to an essential reformulation of the equation 7. We deal now with characters of squares of space group elements  $\chi[\{g|\boldsymbol{\tau}_g + \mathbf{t}\}^2]$ . The  $\boldsymbol{\tau}_g$  is a non-primitive translation associated with operator  $g$  which essentially belongs to the point group  $G_0(\mathbf{k})$ ,  $\mathbf{t}$  is primitive translation, and summation is over these  $g$ 's which transform  $\mathbf{k}$  into  $-\mathbf{k}$ . The  $\mathbf{k}$  is the first wave vector of the star  $\{\mathbf{k}\}$ . The total space group  $G$  contains all groups of all members of the star and it can be decomposed in terms of  $G(\mathbf{k})$ :

$$G = G(\mathbf{k}) + \{\varphi_2 | \boldsymbol{\tau}_2\}G(\mathbf{k}) + \{\varphi_2 | \boldsymbol{\tau}_2\}G(\mathbf{k}) + \dots + \{\varphi_\sigma | \boldsymbol{\tau}_\sigma\}G(\mathbf{k}) \quad (8)$$

We reserve the subscript  $\sigma$  for the coset representatives  $\{\varphi_\sigma | \boldsymbol{\tau}_\sigma\}$ . And the members of a star is obtained by symmetry operators  $\varphi$  of the point group  $G_0(\mathbf{k})$ .

$$\{\mathbf{k}\} = \mathbf{k}_1 = \mathbf{k}_2 = \varphi_2 \mathbf{k} \dots \mathbf{k}_s = \varphi_s \mathbf{k} \quad (9)$$

The  $\mathbf{k}$  is the first wave vector of the star in the fundamental domain of the BZ. The characters of 230 space groups of these first wave vectors are tabulated [1]. Evaluating the character of the squared operators we obtain:

**Table 1.** Real and complex irreducible representations of 32 crystallographic double point groups. Kronecker Product Tables. CDML [1]

Group Representation $\Gamma_j$	case (a) j	case (b) j	case (c) j
$O_h$	1+,2+,3+,4+,5+ 1-, 2-, 3-, 4-, 5-	6+,7+,8+,7-,8-,9-	
$O$	1,2,3,4,5		6,7,8
$T_d$	1,2,3,4,5		6,7,8
$T_h$	1+,4+,1-,4-	2+,3+,2-,3-	5+,6+,7+,5-,4-,5-
$T$	1,4	2,3	5,6,7
$D_{4h}$	1	2+,3+,4+,5+,2-,3-,4-,5-	6+,7+,6-,7-
$C_{4h}$	1+,2+,1-,2-	3+,4+,3-,4-	5+,6+,7+,8+,5-,6-,7-,8-
$C_{4v}$	1,2,3,4		6,7
$D_4$	1,2,3,4,5		6,7
$C_4$	1,2	3,4,5,6,7,8	
$S_4$	1,2	3,4,5,6,7,8	
$D_{2d}$	1,2,3,4,5		6,7
$D_{2h}$	1+,2+,3+,4+,1-,2-,3-,4-		5+,5-
$C_{2h}$	1+,2+,3+,4+,1-,2-,3-,4-		5+,5-
$C_{2v}$	1,2,3,4		5-
$D_2$	1,2,3,4		5
$C_2$	1,2	3,4	
$D_{6h}$	1+,2+,3+,4+,5+,6+, 1-,2-, 3-, 4-, 5-, 6-		7+,8+,9+,7-,8-,9-
$C_{6h}$	1+,2+,3+,4+,5+,6+, 1-, 2-, 3-, 4-, 5-, 6-	7+,8+,9+,10+,11+,12 7-, 8-, 9-, 10-, 11-, 12-	
$C_{6v}$	1,2,3,4,5,6		7,8,9
$D_6$	1,2,3,4,5,6		7,8,9
$D_{3h}$	1,2,3,4,5,6		7,8,9
$D_{3d}$	1+,2+,3+,1-,2-,3-	4+,5+,4-,5-,	6+,6-
$C_6$	1,2	3,4,5,6,7,8,9,10,11,12	
$C_{3h}$	1,2	3,4,5,6,7,8,9,10,11,12	
$C_{3v}$	1,2,3	4,5	6
$D_3$	1,2,3	4,5	6
$C_i$	1+,2+,1-,2-		
$C_3$	1,5	2,3,4,6	
$C_2$	1,2	3,4	
$C_s$	1,2	3,4	
$C_1$	1		

$$\chi\{[g|\tau_g]^2\} = \chi\{g^2|\tau_g + g\tau_g\} = \chi\{g^2|\tau'_g + \tau_g + g\tau_g - \tau'_g\}$$

$$= \chi\{\epsilon|\mathbf{t}_0\}\chi\{g^2|\tau'_g\} = \exp(i\mathbf{k}\mathbf{t}_0)\chi\{g^2|\tau'_g\}, \quad (10a)$$

$$\mathbf{t}_0 \equiv \tau_g + g\tau_g - \tau'_g, \quad (10b)$$

where  $\tau'_g$  is known non-primitive translation associated with the operator  $g$ ,  $\epsilon$  is the identity operator and  $\mathbf{t}_0$  is to be calculated from equation (10b). The criterion for real and complex irrps of space groups becomes:

$$(|G|/|G(\mathbf{k})|)\sum_{g \in G(\mathbf{k})} \exp(i\mathbf{k}\mathbf{t}_0)\chi\{g^2|\tau'_g\}\delta_{\mathbf{k}, -g\mathbf{k}} = 1 \text{ or } 0 \quad (11)$$

where the summation is performed over  $g^2 \subset G(\mathbf{k})$  such that  $g\mathbf{k} = -\mathbf{k}$  and the  $|G|/|G(\mathbf{k})|$  is the number of symmetry elements in the small wave vector group  $G(\mathbf{k})$ . The formula differs from Bir and Picus [9 page 166 equation (18.32)]. We have utilized the CDML tables where the characters  $\chi\{g|\tau_g\}$  of the irrps of 230 space groups are explicitly listed and therefore the characters of  $\{g^2|\tau_g\}$  are chiefly available.

Using equation (11) and CDML tables we have tested all reps of the high symmetry points and lines of the ZnO space group  $C_{6v}^4$ . The results are:

- (a)  $\Gamma_{1,2,3,4,5,6}, M_{1,2,3,4}, K_{1,2,3}, \Sigma_{1,2}, T_{1,2}, H_3$ . Real reps. No extra degeneracy
- (b)  $A_{1,2,3,4,5,6}, \Delta_{1,2,3,4,5,6}, H_{1,2}, L_{1,2,3,4}, U_{1,2,3,4}, P_{1,2,3}, S_{1,2}$ . Complex reps.
- (c)  $R_{1,2}$ . Complex reps.

In cases (b) and (c) the extra  $TR$  degeneracy arises and the “ons” are classified according to the “joint” or “stick” reps:  $D \oplus D^*$ .

**Table 2.** Vector representation of hexagonal crystallographic point groups.

1	$E$	$h_1$	$x, y, z$	1 0 0 0 1 0 0 0 1	13	$I$	$h_{13}$	$-x, -y, -z$	-1 0 0 0 -1 0 0 0 -1
2	$C_6^+$	$h_2$	$x-y, x, y$	1 -1 0 1 0 0 0 0 1	14	$S_3^-$	$h_{14}$	$-x+y, -x, -z$	-1 1 0 -1 0 0 0 0 -1
3	$C_3^+$	$h_3$	$-y, x-y, z$	0 -1 0 1 -1 0 0 0 1	15	$S_5^-$	$h_{15}$	$y, -x+y, -z$	0 1 0 -1 1 0 0 0 -1
4	$C_2$	$h_4$	$-x, -y, z$	-1 0 0 0 -1 0 0 0 1	16	$\sigma_h$		$x, y, -z$	1 0 0 0 1 0 0 0 -1
5	$C_3^-$	$h_5$	$-x+y, -x, z$	-1 1 0 -1 0 0 0 0 1	17	$S_6^+$		$x-y, x, -z$	1 -1 0 1 0 0 0 0 -1
6	$C_6^-$	$h_6$	$y, -x+y, z$	0 1 0 -1 1 0 0 0 1	18	$S_3^+$		$-y, x-y, -z$	0 -1 0 1 -1 0 0 0 -1
7	$C_{21}''$	$h_9$	$x-y, -y, -z$	1 -1 0 0 -1 0 0 0 -1	19	$\sigma_{v1}$		$-x+y, y, z$	-1 1 0 0 1 0 0 0 1
8	$C_{22}'$	$h_{10}$	$x, x-y, -z$	1 0 0 1 -1 0 0 0 -1	20	$\sigma_{d2}$			-1 0 0 -1 1 0 0 0 1
9	$C_{23}''$	$h_{11}$	$y, x, -z$	0 1 0 1 0 0 0 0 -1	21	$\sigma_{v3}$			0 -1 0 -1 0 0 0 0 1
10	$C_{21}'$	$h_{12}$	$-x+y, y, -z$	-1 1 0 0 1 0 0 0 -1	22	$\sigma_{d1}$			1 -1 0 0 -1 0 0 0 1
11	$C_{22}''$	$h_7$	$-x, -x+y, -z$	-1 0 0 -1 1 0 0 0 -1	23	$\sigma_{v2}$			1 0 0 1 -1 0 0 0 1
12	$C_{23}'$	$h_8$	$-y, -x, -z$	0 -1 0 -1 0 0 0 0 -1	24	$\sigma_{d3}$			0 1 0 1 0 0 0 0 1

Up to now we have considered only single valued reps of space groups (spin excluded). The inclusion of spin leads to the double valued reps. The criterion (equation 11) is also valid for spinors. In general, in order to perform calculation using equation (11) we must consider systems with (i) integral and (ii) half-odd-integral spin. Combination of the three cases (a), (b), and (c) with (i) and (ii) result in additional six possibilities those can expressed as follows:

- No extra degeneracy in case a(i) and c(ii),
- Doublet degeneracy in cases b(i), b(ii), a(ii) and c(i),

- In table 3, we discuss points  $A, \Delta, M, L, H, K$ , and lines  $\Lambda, \Sigma$ .

In here we have considered spinor reps, case (ii)-1/2 spin, of points  $\Gamma, A, H, K, M, L$ , and  $\Delta$  line. The characters of spinor reps of the double groups have been taken from CDML tables. Using the equation (11) we have obtained following results:

- Case a(ii) no  $TR$  degeneracy:  $\Gamma_{6,7,8}$
- Case b(ii) doublet degeneracy:  $\Delta_{7,8,9}, H_{4,5}, K_{4,5}$ . Classification of states:  

$$\Delta_7 \oplus \Delta_7^*, \Delta_8 \oplus \Delta_8^*, \Delta_9 \oplus \Delta_9^*, H_4 \oplus H_4^*, K_4 \oplus K_4^*$$
- Case c(ii) no  $TR$  degeneracy:  $A_{7,8,9}, H_6, K_6$ .

**Table 3.** Characters of the irreducible  $A, \Delta, M, L, H, K, \Sigma$  and  $\Lambda$  representations.

Space Group  $C_{6v}^4(P6_3/mc)$ . CDML symmetry elements labelling:  $\{g|\tau_g\}$  of  $G^{k_A}/T$

$\{g \tau_g\}$	1	2.1	3	4.1	5	6.1	19	20.1	21	22.1	23	24.1
$A_1$	1	$i$	1	$i$	1	$i$	1	$i$	1	$i$	1	$i$
$A_2$	1	$i$	1	$i$	1	$i$	-1	- $i$	-1	- $i$	-1	- $i$
$A_3$	1	- $i$	1	- $i$	1	- $i$	-1	$i$	-1	$i$	-1	$i$
$A_4$	1	- $i$	1	- $i$	1	- $i$	1	- $i$	1	- $i$	1	- $i$
$A_5$	1 0	$i w^* 0$	$w 0$	$i 0$	$w^* 0$	$i w 0$	0 - $i$	0 - $w^*$	0 - $i w$	0 - $i$	0 - $i w$	0 - $w$
	0 1	0 $i w$	0 $w^*$	0 $i$	0 $w$	0 $i w^*$	$i 0$	$w 0$	$i w^* 0$	$i 0$	$i w 0$	$w^* 0$
$A_6 = A_5^*, A_4 = A_1^*, A_2 = A_3^*$												
$\{g \tau_g\}^2$	1	$3t_0$	5	$1t_0$	3	$5t_0$	1	$1t_0$	1	$1t_0$	1	$1t$
Characters of $\{g \tau_g\}^2, t_0 = \{E 001\}, \exp(i\mathbf{k}_A t_0) = \exp[i(0,0,1/2)(0,0,1)] 2\pi = e^{i\pi} = -1$												
$A_{1,2,3,4}$	1	$1(-1)$	1	$1(-1)$	1	$1(-1)$	1	$1(-1)$	1	$1(-1)$	1	$1(-1)$
$A_5$	2	$(w+w^*)(-1)$	$(w^*+w)$	$2(-1)$	$(w+w^*)$	$(w^*+w)(-1)$	2	$2(-1)$	2	$2(-1)$	2	$2(-1)$
$A_6$	2	$(w^*+w)(-1)$	$(w+w^*)$	$2(-1)$	$(w^*+w)$	$(w+w^*)(-1)$	2	$2(-1)$	2	$2(-1)$	2	$2(-1)$

$A_{1,2,3,4,5,6}$  case (b)

$G^{k_A}/T$

$\{g \tau_g\}$	1	2.1	3	4.1	5	6.1	19	20.1	21	22.1	23	24.1
$\Delta_1$	1	$1.T$	1	$1.T$	1	$1.T$	1	$1.T$	1	$1.T$	1	$1.T$
$\Delta_2$	1	$1.T$	1	$1.T$	1	$1.T$	-1	- $1.T$	-1	- $1.T$	-1	- $1.T$
$\Delta_3$	1	- $1.T$	1	- $1.T$	1	- $1.T$	-1	$1.T$	-1	$1.T$	-1	$1.T$
$\Delta_4$	1	- $1.T$	1	- $1.T$	1	- $1.T$	1	- $1.T$	1	- $1.T$	1	- $1.T$
$\Delta_5$	1 0	$T w^* 0$	$w 0$	$T 0$	$w^* 0$	$T w 0$	0 $T^2$	0 $T w^*$	0 - $w T^2$	0 $T$	0 - $w^* T^2$	0 $w T$
	0 1	0 $T w$	0 $w^*$	0 $T$	0 $w$	0 $T w^*$	$T^2 0$	$T w 0$	$w^* T^2 0$	$T 0$	$w T^2 0$	$w^* T 0$
$\Delta_6 = \Delta_5^*, \Delta_4 = \Delta_1^*, \Delta_2 = \Delta_3^*$												
$w = \exp(2\pi i/3), T = \exp(i\pi\alpha)$												
For $\Delta$ there is no point group operation $g \in C_{6v}$ which transforms $\mathbf{k}_\Delta$ into $-\mathbf{k}_\Delta$ . $\Delta_{1,2,3,4,5,6}$ case (b)												

$G^{k_M}/T$					$G^{k_L}/T$				
$\{g \tau_g\}$	1	4.1	20.1	23	$\{g \tau_g\}$	1	4.1	20.1	23
$M_1$	1	1	1	1	$L_1$	1	$i$	$i$	1
$M_2$	1	1	-1	-1	$L_2$	1	$i$	- $i$	-1
$M_3$	1	-1	1	-1	$L_3$	1	- $i$	$i$	-1
$M_4$	1	-1	-1	1	$L_4$	1	- $i$	- $i$	1
$\{g \tau_g\}^2$	1	$\{1 0,0,1\}$	$\{1 0,0,1\}$	1	$\{g \tau_g\}^2$	1	$\{1 0,0,1\}$	$\{1 0,0,1\}$	1
$\exp(i\mathbf{k}_M \mathbf{t}) = \exp[i(1/2,0,0)(0,0,1)] 2\pi = 1$					$\exp[i(\mathbf{k}_L \mathbf{t})] = \exp[i(1/2,0,1/2)(0,0,1)] = -1$				
Characters of $\{g \tau_g\}^2$									
$M_{1,2,3,4}$	1	1	1	1	$L_{1,2,3,4}$	1	$1(-1)$	$1(-1)$	1
case (a)					case (b)				

$G^{k_H} / T$							$G^{k_K} / T$						
$\{g \tau_g\}$	1	3	5	20.1	22.1	24.1	$\{g \tau_g\}$	1	3	5	20.1	22.1	24.1
$H_1$	1	1	1	$i$	$i$	$i$	$K_1$	1	1	1	1	1	1
$H_2$	1	1	1	$-i$	$-i$	$-i$	$K_2$	1	1	1	-1	-1	-1
$H_3$	2	-1	-1	0	0	0	$K_3$	2	-1	-1	0	0	0
$\{g \tau_g\}^2$	1	5	3	$\{1 0,0,1\}$	$\{1 0,0,1\}$	$\{1 0,0,1\}$	$\{g \tau_g\}^2$	1	5	3	$\{1 0,0,1\}$	$\{1 0,0,1\}$	$\{1 0,0,1\}$
$\exp(i\mathbf{k}_H \mathbf{t}) = \exp[i(1/3, 1/3, 1/2)(001)]2\pi = -1$							$\exp(i\mathbf{k}_K \mathbf{t}) = \exp[i(1/3, 1/3, 0)(001)]2\pi = 1$						
Characters of $\{g \tau_g\}^2$													
$H_{1,2}$	1	1	1	1(-1)	1(-1)	1(-1)	$K_{1,2}$	1	1	1	1	1	1
$H_3$	2	-1	-1	2(-1)	2(-1)	2(-1)	$K_3$	2	-1	-1	2	2	2
$H_{1,2}$ case (b), $H_3$ case (c)							$K_{1,2,3}$ case (a)						

$G^{k_A} / T$			$G^{k_E} / T$		
$\{g \tau_g\}$	1	24.1	$\{g \tau_g\}$	1	23
$\Lambda_1$	1	1	$\Sigma_1$	1	1
$\Lambda_2$	1	-1	$\Sigma_2$	1	-1
$\{g \tau_g\}^2$	1	$\{1 0,0,1\}$	$\{g \tau_g\}^2$	1	1
$\exp(i\mathbf{k}_A \mathbf{t}) = \exp[i(\alpha, \alpha, 0)(0,0,1)]2\pi = 1$			$\exp(i\mathbf{k}_E \mathbf{t}) = \exp[i(\alpha, 0, 0)(0,0,1)]2\pi = 1$		
Characters of $\{g \tau_g\}^2$					
$\Lambda_{1,2}$	1	1	$\Sigma_{1,2}$	1	1
case (a)			case (a)		

1 =  $E$ , 2.1 =  $\{C_6^+|0,0,1/2\}$ , 3 =  $\{C_3^+\}$ , 4.1 =  $\{C_2|0,0,1/2\}$ , 5 =  $\{C_3^-\}$ , 6.1 =  $\{C_6^-|0,0,1/2\}$   
19 =  $\{\sigma_{v1}\}$ , 20.1 =  $\{\sigma_{d2}|0,0,1/2\}$ , 21 =  $\{\sigma_{v3}\}$ , 22.1 =  $\{\sigma_{d1}|0,0,1/2\}$ , 23 =  $\{\sigma_{v2}\}$ , 24.1 =  $\{\sigma_{d3}|0,0,1/2\}$

### 3. Examples. Points $M$ and $L$

In here we test the irrps of ZnO of the high symmetry points  $L$ ,  $G(\mathbf{k}_L)$  and  $M$ ,  $G(\mathbf{k}_M)$ .

Coordinates are;  $\mathbf{k}_M \approx (1/2, 0, 0)$  and  $\mathbf{k}_L \approx (1/2, 0, 0)$ . The symmetry operators of the  $G(\mathbf{k}_M)/T$  and  $G(\mathbf{k}_L)/T$  are 1 =  $E$ , 4.1 =  $\{C_2|001/2\}$ , 20.1 =  $\{\sigma_{d2}|001/2\}$ , 23 =  $\{\sigma_{v2}\}$

Let's calculate the square of symmetry element 4.1 using the equations (10a,b)

$$\begin{matrix} & & & & 1 & -1 & 0 \\ \{4.1\}^2 = \{C_2^2|001/2 + C_2(001/2)\}, & C_2(001/2) = & \begin{matrix} 1 & 0 & 0 \\ 0 & 0 & 1 \end{matrix} & (001/2) = & (0,0,1/2). \end{matrix}$$

Therefore:  $\{C_2^2|001/2 + 001/2\} = \{E|001\}$ , and similarly for  $\{20.1\}^2$  and  $\{23\}^2$ . Thus the characters of the squared operators for point  $M$  and  $L$  are

$$\chi\{E^2\} = \chi\{E\}, \chi\{(4.1)^2\} = \chi\{E|001\}, \chi\{(20.1)^2\} = \chi\{E|001\}, \chi\{(23)^2\} = \chi\{E\}$$

For matrices of the vector representation for hexagonal groups see table 2. Since the  $\mathbf{k}_M$  and  $\mathbf{k}_L$  have different coordinates the factor  $\exp(i\mathbf{k}\mathbf{t})$  will differ. For point  $M$ , we have

$$\exp(i\mathbf{k}_M \mathbf{t}): \text{for } \chi\{(4.1)^2\} \text{ and } \chi\{(20.1)^2\} \text{ is: } \exp[i(1/2, 0, 0)(0, 0, 1)2\pi] = \exp(0) = 1.$$

Therefore, the characters of the squared operators of point  $M$  are:

$$\chi\{E^2\} = \chi\{E\}, \chi\{(4.1)^2\} = \chi\{E\}, \chi\{(20.1)^2\} = \chi\{E\}, \chi\{(23)^2\} = \chi\{E\}.$$

For point  $L$ , we have

$$\exp(i\mathbf{k}_L \mathbf{t}): \text{for } \chi\{(4.1)^2\} \text{ and } \chi\{(20.1)^2\} \text{ is: } \exp[i(1/2, 0, 1/2)(0, 0, 1)2\pi] = \exp(i\pi) = -1.$$

Therefore, the characters of the squared operators of point  $L$  are:

$$\chi\{E^2\} = \chi\{E\}, \chi\{(4.1)^2\} = -1\chi\{E\}, \chi\{(20.1)^2\} = -1\chi\{E\}, \chi\{(23)^2\} = \chi\{E\}.$$

See table 2 for  $G(\mathbf{k}_M)/T$  and  $G(\mathbf{k}_L)/T$ .

From equation (8) we obtain the star for  $\mathbf{k}_M$  and  $\mathbf{k}_L$

$$G = \{1\}G(\mathbf{k}_M) + \{2.1\}G(\mathbf{k}_M) + \{3\}G(\mathbf{k}_M),$$

where  $\{1\} = \{E\}$ ,  $\{2.1\} = \{C_6^+|0,0,1/2\}$ ,  $\{3\} = \{C_3^+\}$  are the coset representatives by means of those the stars  $\{\mathbf{k}_M\}$  and  $\{\mathbf{k}_L\}$  are obtained:  $E\mathbf{k}_M = 1\mathbf{k}_M$  (1/2,0,0),  $(C_6^+)\mathbf{k}_M = 2\mathbf{k}_M$  (1/2,1/2,0),  $C_3^+\mathbf{k}_M = 3\mathbf{k}_M$  (0,1/2,0) and for  $\{\mathbf{k}_L\}$  we have  $E\mathbf{k}_L = 1\mathbf{k}_L$  (1/2,0,1/2),  $C_6^+\mathbf{k}_L = 2\mathbf{k}_L$  (1/2,1/2,1/2),  $C_3^+\mathbf{k}_L = 3\mathbf{k}_L$  (0,1/2,1/2). The coset representatives are useful in the determination of the full induced irrps of  $G\{\mathbf{k}\}$  [10] and in the performing the summation in equation (11). Using the calculated coset representatives we have proceeded (for  $M$  and  $L$  points) both ways and our results are in agreement with those obtained in here using characters of the small irrps tabulated.

#### 4. The effect of time reversal symmetry on vibrational states in wurtzite structure crystals with $C_{6v}^4$ space group

Before going into discussion of experimental results we recall general utilization of group theory related to phonons in any crystal with well establish space group [11]. The Lattice Mode Representation (LMR) [12] of a crystal provides an exact number of primary (first order – non-interacting phonons) originating from high symmetry point and lines of a BZ and also their symmetries (irrps, degeneracies). For example, for ZnO we have following symmetry allowed vibrational modes:  $(2\Gamma_1, 2\Gamma_4, 2\Gamma_5, 2\Gamma_6)$ ,  $(2A_1, 2A_4, 2A_5, 2A_6)$ ,  $(2\Delta_1, 2\Delta_4, 2\Delta_5, 2\Delta_6)$ ,  $(2H_1, 2H_2, 2H_3)$ ,  $(2P_1, 2P_2, 2P_3)$ ,  $(2K_1, 2K_2, 2K_3)$ ,  $(4L_1, 2L_2, 2L_3, 4L_4)$ ,  $(4M_1, 2M_2, 2M_3, 4M_4)$ ,  $(4U_1, 2U_2, 2U_3, 4U_4)$ ,  $(8R_1, 4R_2)$ ,  $(8\Sigma_1, 4\Sigma_2)$ ,  $(6Q_1, 6Q_2)$ ,  $(6S_1, 6S_2)$ ,  $(6\Lambda_1, 6\Lambda_2)$ , and  $(6T_1, 6T_2)$  [11]. Knowing these symmetries and using compatibility relations along high symmetry lines and points the group theoretical assignment of phonons follows. Phonons assignment in ZnO, GaN, and related compounds with the  $C_{6v}^4$  space group is presented on figure 1 in [11].

##### 4.1. Experimental phonon dispersion curves in ZnO. Assignment

Thoma and Hewat [4,5] considered lattice dynamics of ZnO by means of inelastic neutron scattering. Figure 1 in [4,5] shows the calculated and measured phonon dispersion curves for ZnO. Our phonon assignment for GaN (presented on figure 1 in [4,5]) is valid also for phonons in ZnO. According to our calculations, the  $\Delta$  and  $A$  phonons are influenced by the  $TR$  symmetry. However, on both figures 1 in [4,5] there is no group theoretical assignment of vibrational modes. We have shown that at point  $A$  and axis  $\Delta$  the representations spanned by the modes are  $2A_1 \oplus 2A_4 \oplus 2A_5 \oplus 2A_6$  and  $2\Delta_1 \oplus 2\Delta_4 \oplus 2\Delta_5 \oplus 2\Delta_6$ , respectively. In other words, there are eight  $A$ 's and eight  $\Delta$ 's modes. We also know that at point  $\Gamma$  there are also eight modes of  $2\Gamma_1, 2\Gamma_4, 2\Gamma_5, 2\Gamma_6$  symmetries. The presence of  $TR$  symmetry (at  $A$  and  $\Delta$ ) requires classification of modes according to  $A \oplus A^*$ ,  $\Delta \oplus \Delta^*$  reps. Using the compatibility relations the resulting mode's assignment is:

(i) Point  $\Gamma$ , from the bottom to the top:  $\Gamma_1 \oplus \Gamma_5$ ,  $\Gamma_6$ ,  $\Gamma_4$ ,  $\Gamma_5$ ,  $\Gamma_6$ ,  $\Gamma_4$ , and  $\Gamma_1$ .

(ii) Point  $A$ , from the bottom to the top:  $A_5 \oplus A_5^*$ ,  $A_1 \oplus A_1^*$ ,  $A_5 \oplus A_5^*$ ,  $A_1 \oplus A_1^*$ .

(iii) Line  $\Delta$ : the dispersion curves connect the points  $\Gamma$  and  $A$  when going from the bottom to the top on  $A$  axis side:  $\Delta_5, \Delta_5^*$ ,  $\Delta_1, \Delta_1^*$ ,  $\Delta_5, \Delta_5^*$ ,  $\Delta_1^*$ , and  $\Delta_1$ .

From reps provided in here follows that  $A_1^* = A_4$ , and  $A_5^* = A_6$ , and  $\Delta_1^* = \Delta_4$ ,  $\Delta_5^* = \Delta_6$ , which is consistence with the number of modes at  $\Gamma$ ,  $A$ , and  $\Delta$  and with their symmetries obtained independently from Lattice Mode Representation. Figure 1 displays the schematic dispersion curves of  $\Gamma$ – $\Delta$ – $A$  region of the BZ subjected to  $TR$  symmetry for ZnO in terms of ‘‘joint’’ reps. For simplicity, we used straight lines for connectivity. Generally, the frequencies of the modes at  $\Gamma$ ,  $\Delta$  and  $A$  point may shift while going from compound to compound (for instance from ZnS to BeO, all with the wurtzite structure,  $C_{6v}^4/T$  group), but the connecting dispersion curves between  $\Gamma$  and  $A$  point will be kept by



$\Delta$ 's experimental phonon data. The shifting may cause more accidental degeneracy. The existence of experimentally measured modes, those “generate” dispersion curves  $\Delta_5$ ,  $\Delta_6$ ,  $\Delta_1$ ,  $\Delta_4$  and four phonons on  $A$  axis  $2(A_5 \oplus A_6)$ ,  $2(A_1 \oplus A_4)$  evidently proves the presence of the Time Reversal symmetry in wurtzite crystals. Figure 1 displays the schematic dispersion curves  $\Gamma - \Delta - A$  region of BZ subjected to  $TR$  symmetry in wurtzite crystal in term of “joint” reps.

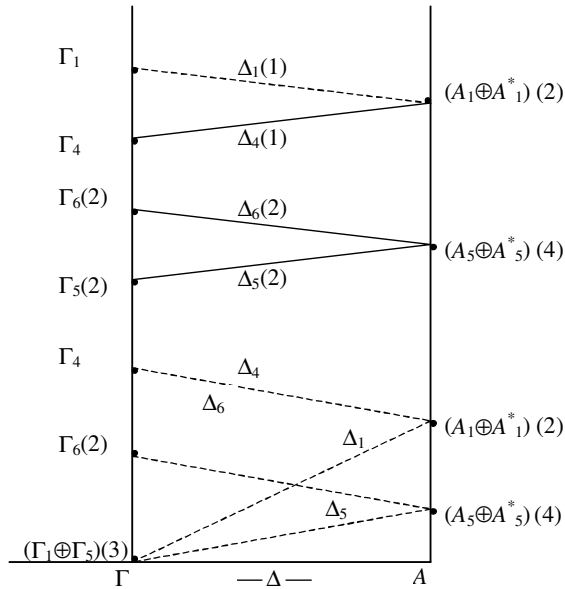


**Figure 1.** Assignment of phonons in ZnO, GaN, CdS, BeO, ZnS, CdSe influenced by time reversal symmetry. Numbers in brackets indicate the degree of degeneracy.

## 5. Effect of time reversal symmetry on electronic band structure and optical transitions in wurtzite crystals with $C_{6v4}$ space group. Selection rules GaN band structure

Since the states of electrons in conduction and holes in valence bands are classified according to the irrps of the factor group of the wave vectors in the fundamental BZ domain (first vectors of a stars) the effect of  $TR$  must be taken into account. The wurtzite BZ and the calculated LDA energy bands of GaN are given, (see figure 2 and figure 4 pages 308 and 310 in [13]). On the figure 4 the classification of states is only in terms of single valued reps of the space group  $C_{6v}^4$ . It means that spin of electron and holes has been excluded. However, in GaN there is an appreciable spin orbit interaction [13.p.307] that splits the top of the valence  $\Gamma_{1,6}$  ( $\Gamma_1 \oplus \Gamma_6$ )  $\otimes D_{1/2}$  band onto  $\Gamma_9 + \Gamma_7$  and  $\oplus \Gamma_7$  the later being split by crystalline field. Therefore, the energy band structure presented on figure 4 [13] may not correspond to the true one. Nevertheless,  $TR$  symmetry has been taken into account. For example, the top of the valence band at point  $A$  (figure 4) is described by (5, 6) numbers, which means  $A_5 \oplus A_5^*$  state  $TR$  degenerate. One of the lower valence band state at  $K$  point is classified by single valued irrps  $K_3$  (two-dimensional). Inclusion of spin results in Kronecker Product  $(KP) K_3 \otimes D_{1/2}$  sixfold degenerate spinor state, which must be decomposed onto double valued  $(K_{4,5,6})$  irrps of  $K$ . The  $D_{1/2}$  is the  $2 \times 2$  spin matrix. Generally, all states of holes and electrons will be classified according to their spinor reps when spin included. To our best knowledge the electronic band structure of GaN and many other novel compounds do not include spin. Using compatibility relations and spin matrix we have described the GaN energy band (Fg.4) in terms of spinor states those are frequently subjected to  $TR$  effect, as showed in section 2d. Our results will be discussed elsewhere.

### 5.1. Selection rules

In here we briefly discuss additional conditions that invariance under  $TR$  imposes on the matrix elements of an operator  $V$ . Our discussion will be related to selection rules of some optical transitions between  $TR$  influenced states in GaN. In general we have:

$$\langle \varphi_f V \varphi_i \rangle = \int \varphi_f^* V \varphi_i d\mathbf{r}, \quad (12a)$$

$$\langle K \varphi_f | K \varphi_i \rangle = \langle \varphi_f \varphi_i \rangle^*, \quad (12b)$$

$$\langle \varphi_f V \varphi_i \rangle^* = \langle K \varphi_f, K V \varphi_i \rangle = \langle K \varphi_f, K V K^{-1} K \varphi_i \rangle, \quad (12c)$$

where the  $\varphi_i$ ,  $\varphi_f$ ,  $V$  and  $K$  are initial and, final states, perturbation and Time Reversal operators, respectively. The  $K\varphi_i$  and  $K\varphi_f$  yield complex irrps  $D_i^*$  and  $D_f^*$  between those transition takes place. It is sufficient to consider only possible  $KPs$ :  $D_i^* \otimes D_f^*$  and find out whether in their decomposition is a rep according to which the perturbation  $V$  transforms. The Kronecker Products of all irrps of 230 space groups are tabulated, CDML [1]. However, the  $TR$  symmetry has not been included. Therefore, for all irrps satisfying cases (b) and (c) of Herring's criterion the selection rules must be computed. The formal theory involved in such cases will be considered elsewhere. In here we discuss only practical transitions involved in  $UV$  reflectivity of GaN [14]. There are two cases concerning the effect of the  $TR$  on selection rules regarding the CDML tables. If a complex irrps satisfying (b) or (c) cases are in the set of irrps of a space group tabulated then selection rules can be still extracted from the CDML tables. For instance, at point A in ZnO we have states  $A_1 \oplus A_1^*$ ,  $A_2 \oplus A_2^*$ ,  $A_3 \oplus A_3^*$ ,  $A_4 \oplus A_4^*$ ,  $A_5 \oplus A_5^*$  and  $A_6 \oplus A_6^*$ . However, from inspection of the tables we conclude that:  $A_1^* = A_4$ ,  $A_2^* = A_3$ ,  $A_5^* = A_6$ . For transition between levels  $A_{5,6}$  and  $A_{1,3}$  (5.94eV), [14. Table III p. 13 529]) one reads

$$(A_5 \oplus A_6) \otimes (A_1 \oplus A_3) = (A_5 \oplus A_1) \otimes (A_5 \oplus A_3) \oplus (A_6 \oplus A_1) \otimes (A_6 \oplus A_3).$$

in Rashba's labelling [15]. The Rashba's  $A_2$  corresponds to  $A_3$  CDML and so  $A_3 - A_4$ ,  $A_4 - A_2$  correspondingly, (see table 4, this paper). The above  $KPs$  are tabulated (vol p). Therefore, in such cases no implications are involved. In this spirit, the selection rules for tabulated transitions (see Table III in [14]) between  $A$ ,  $\Delta$ ,  $L$ ,  $U$ ,  $P'$  levels can still be found in the CDML tables. Nevertheless, considering transitions between  $TR$  degenerate  $K_5$  and  $K_6$  levels (spin included) we have

$$(K_5 \oplus K_5^*) \otimes (K_6 \oplus K_6^*) = K_5 \otimes K_6 \oplus K_5 \otimes K_6^* \oplus K_5^* \otimes K_6 \oplus K_5^* \otimes K_6^*.$$

The rep  $K_5$  is one-dimensional, while  $K_6$  is two-dimensional. Neither  $K_5^*$  nor  $K_6^*$  is in the set of  $K$ 's reps of the  $G(\mathbf{K})$  group. Only the product  $K_5 \otimes K_6$  can be found in the CDML tables. All the other  $KPs$  have to be calculated. Clearly,  $TR$  symmetry results in additional  $KPs$  of complex reps those have to be determined.

**Table 4** Labels of irreducible group  $C_{6v}^4$  representations of the space group (P6<sub>3</sub>/mc)

CDML													Rashba													Lyle et al.									
$\Gamma$	$\Delta$	$A$	$L$	$M$	$U$	$K$	$H$	$P$	$\Sigma$	$\Lambda$	$Q$	$S$	$T$	$R$	$\Gamma$	$\Delta$	$A$	$L$	$M$	$U$	$K$	$H$	$P$	$\Sigma$	$T$	$S$	$S'$	$T'$	$R$	$\Gamma$	$\Delta$	$A$	$K$		
1	1	1	1	1	1	1	1	1	1	1	1	1	1	1	1	1	1	1	1	1	1	1	1	1	1	1	1	1	1	1	1	1	1	1	1
2	2	2	2	2	2	2	2	2	2	2	2	2	2	2	2	2	2	4	4	4	2	2	2	2	2	2	2	2	2	2	2	2	2	2	2
3	3	3	3	3	3	3	3	3							4	4	4	2	2	2	3	3	3												
4	4	4	4	4	4										3	3	3	3	3	3															
5	5	5													5	5	5																		
6	6	6													6	6	6																		

CDML see [1], Rashba see [15], Lyle et al. see [16].

## 6. Conclusions

In this paper we discussed the effect of  $TR$  symmetry on quasi-particles states. We have shown that a presence of  $TR$  in crystals results in modified classification of states, phonon dynamical matrices, energy bands, optical selection rules, and others.

In conclusion: a comprehensive tables of complex irreducible representations of 230 double valued space group are needed. In table 5 we list the most common compounds and their symmetries. The table can be quite useful in making a choose of further investigations of *TR* effect in these compounds.

**Table 5.** Compounds and their symmetries.

$D_{2h}^1$ (Pmmm)	YBa <sub>2</sub> Cu <sub>3</sub> O <sub>7</sub> High Temperature Superconductor (HTS)
$D_{2h}^5$ (Pmma)	Si <sub>2</sub> G <sub>2</sub> Semiconductor Superlattices (SS)
$D_{2h}^{12}$ (Pnmm)	Marcasite structure. FeS <sub>2</sub> and crystals isomorphic to FeS <sub>2</sub> : FeAs <sub>2</sub> , FeP <sub>2</sub> , FeSb <sub>2</sub> , FeSe <sub>2</sub> , FeTe <sub>2</sub> , CoTe <sub>2</sub> , NiAs <sub>2</sub> , etc.
$D_{2h}^{16}$ (Pnma)	MnP
$D_{2h}^{18}$ (Cmca)	Si <sub>2</sub> Ge <sub>4</sub> (SS)
$D_{2h}^{28}$ (Imma)	La <sub>2</sub> CuO <sub>4</sub>
$D_{2d}^5$ (C42m)	(Si) <sub>m</sub> (Ge) <sub>n</sub> : (m + n = 4k: m,n odd ), Si <sub>1</sub> Ge <sub>3</sub> , (GaAs) <sub>1</sub> (AlAs) <sub>1</sub> , (GaAs) <sub>1</sub> (AlAs) <sub>3</sub> , (GaAs) <sub>2</sub> (AlAs) <sub>2</sub> , SS
$D_{2d}^9$ (F42m)	(Si) <sub>m</sub> (Ge) <sub>n</sub> : (m + n = 4k + 2; m, n odd), Si <sub>3</sub> Ge <sub>3</sub> , (GaAs) <sub>1</sub> (AlAs) <sub>2</sub> , (SS)
$D_{4h}^1$ (P4/mmm)	YBa <sub>2</sub> Cu <sub>3</sub> O <sub>6</sub> host material for the HTS: YBa <sub>2</sub> Cu <sub>3</sub> O <sub>6+δ</sub> Tl Ba <sub>2</sub> Ca <sub>n-1</sub> Ca <sub>n</sub> O <sub>2n+3</sub> HTS
$D_{4h}^{14}$ (P4 <sub>2</sub> /mnm)	Rutile type: TiO <sub>2</sub> , and CoF <sub>2</sub> , MnO <sub>2</sub> , PhO <sub>2</sub> , WO <sub>2</sub>
$D_{4h}^{17}$ (I4/mmm)	Bi(Tl) <sub>2</sub> Sr(Ba) <sub>2</sub> Ca <sub>n-1</sub> Cu <sub>n</sub> O <sub>2n+4</sub> HTS
$D_{4h}^{19}$ (I4 <sub>1</sub> /amd)	TiO <sub>2</sub> – anatase. (Si) <sub>m</sub> (Ge) <sub>n</sub> : (m + n = 2k + 1), Si <sub>1</sub> Ge <sub>2</sub> , (SS)
$T_h^6$ (Pa3)	CoS <sub>2</sub> , MnS <sub>2</sub> , NiS <sub>2</sub>
$T_h^7$ (Ia3)	Tl <sub>2</sub> O <sub>3</sub>
$T_d^2$ (F43m)	GaAs, ZnS, AgJ, AlP, CuBr, CuCl, HgS, ZnSe, ZnTe, CdTe
$O_h^1$ (Pm3m)	Cesium chloride structure CsCl, CsBr, CsI, RbCl, TlCl, TlBr, Intermetallic binary compounds LiAg, AlNd, FeAl, FeTi, Compounds of magnesium MgAg, -Sr, -La, -Ce, -Pr, -Au, -Hg, -Tl, of beryllium BeCo, -Cu, -Pd, of copper CuZn and CuPd of zinc ZnAg, -La, -Ce, -Pr, -Au, of thallium TlCa, -b, -I, -Bi, perovskite structure NaNbO <sub>3</sub> , NaTaO <sub>3</sub> , NaWO <sub>3</sub> , CaTiO <sub>3</sub> , KTaO <sub>3</sub> , SrTiO <sub>3</sub> , BaTiO <sub>3</sub> , CaZrO <sub>3</sub> , CaSnO <sub>3</sub> , SrZrO <sub>3</sub> , SrSnO <sub>3</sub> , SrCeO <sub>3</sub> , PbTiO <sub>3</sub> , BaZrO <sub>3</sub> , PbZrO <sub>3</sub> , LaAlO <sub>3</sub> , LaKO <sub>3</sub> , LaCrO <sub>3</sub> , LaMnO <sub>3</sub> , LaFeO <sub>3</sub> , KMnF <sub>3</sub> , KMgF <sub>3</sub> , KNiF <sub>3</sub> , KCdF <sub>3</sub> , RbCaF <sub>3</sub> , RbMnF <sub>3</sub> , CsCaF <sub>3</sub> , CsCdCl <sub>3</sub> , CsCdBr <sub>3</sub> , CsHgCl <sub>3</sub> , CsHgBr <sub>3</sub> , also Mn <sub>3</sub> SnN
$O_h^3$ (Pm3n)	The A – 15 or β - wolfram structure with the formula A <sub>3</sub> B. Materials with the highest transition temperature to the super. Conducting state, Nb <sub>3</sub> Ge, Nb <sub>3</sub> Sn, Nb <sub>3</sub> Al, V <sub>3</sub> Si, V <sub>3</sub> Ga, etc.
$O_h^4$ (Pn3m)	Cuprite Cu <sub>2</sub> O
$O_h^5$ (Fm3m)	NaCl, AgBr, AgCl, BaO, BaS, CaO, CaS, CdO, KBr, KCl, MgO, PbS. Cuprite type Cu, Ag, Au, Al, Ce, Ir, La, Ni, Pd, Pb, Sr, Th etc. Fluoride type CaF <sub>2</sub> , BaF <sub>2</sub> , UO <sub>2</sub> , ZrO <sub>2</sub> , SrCl <sub>2</sub> , K <sub>2</sub> O, K <sub>2</sub> S, Li <sub>2</sub> O, Li <sub>2</sub> S, Na <sub>2</sub> O.
$O_h^6$ (Fm3c)	The rare compounds of the KTiBr <sub>4</sub> x 2H <sub>2</sub> O type. Alloys: NaZn <sub>13</sub> , KZn <sub>13</sub> , KCd <sub>13</sub> , CaZn <sub>13</sub> , ZrBe <sub>13</sub> , Ube <sub>13</sub> .
$O_h^7$ (Fd3m)	Si, Ge, diamond, β - form SiO <sub>2</sub> , spinel Al <sub>2</sub> MgO <sub>4</sub>
$O_h^8$ (Fd3c)	Voltaits, (NH <sub>4</sub> ) <sub>2</sub> Fe <sup>II</sup> Fe <sup>III</sup> <sub>4</sub> (SO <sub>4</sub> ) <sub>12</sub> · 18H <sub>2</sub> O K <sub>2</sub> (Fe <sup>III</sup> , Al) <sub>4</sub> Zn <sub>5</sub> (SO <sub>4</sub> ) <sub>12</sub> · 18H <sub>2</sub> O Rb <sub>2</sub> Fe <sup>II</sup> Fe <sup>III</sup> <sub>4</sub> (SO <sub>4</sub> ) <sub>12</sub> · 18H <sub>2</sub> O, Tl <sub>2</sub> (Fe <sup>III</sup> , Al) <sub>4</sub> Zn <sub>5</sub> (SO <sub>4</sub> ) <sub>12</sub> · 18H <sub>2</sub> O
$O_h^9$ (Im3m)	Metallic elements Li, Na, K, Ba, V, Nb, Ta, α - Cr, Mo, α - W, α - Fe, and Eu also C <sub>2</sub> Cl <sub>6</sub>
$O_h^{10}$ (Ia3d)	Garnets. Calcium aluminium orthosilicate Ca <sub>3</sub> Al <sub>2</sub> (SiO <sub>4</sub> ) <sub>3</sub> , HoGaG, ErGaG, TmGaG, YbGaG, YbAlG, LuAlG, DyAlG, DyGaG, R <sub>3</sub> Al <sub>5</sub> O <sub>12</sub> , Tm <sub>3</sub> Ga <sub>2</sub> (GaO <sub>4</sub> ) <sub>3</sub> , TbAlG, YIG, TblG, GdlG, LuGaG, DyIG, ErIG
$D_3^4$ (P3 <sub>1</sub> 21)	Sulfurdioxide SiO <sub>2</sub> , α - quartz structure, selenium
$D_{3d}^3$ (P3m1)	CdI <sub>2</sub> , La <sub>2</sub> O <sub>3</sub>
$D_{3d}^6$ (R3c)	CaCO <sub>3</sub> , CdCO <sub>3</sub> , FeCO <sub>3</sub> , MgCO <sub>3</sub> , MnCO <sub>3</sub> , NaNO <sub>3</sub> , ZnCO <sub>3</sub> . Corundum: α - Al <sub>2</sub> O <sub>3</sub> (sapphire)
$D_{6h}^4$ (P6 <sub>3</sub> /mmc)	β - ice, NiAs – structure, CoS, FeS, CrS, CuSn, NiSb, Mg, Ba, Cd, La, Nd, Y, Zn
$C_{6v}^4$ (P6 <sub>3</sub> mc)	ZnS – wurtzite, BeO, CdS, ZnO, GaN, 2H-SiC, 4H-SiC, 6H-SiC, 8H-SiC

**References**

- [1] Cracknell A P, Davies B L, Miller S C and Love W F 1979, *Kronecker Product Tables vol.1-4 IFI* (New York, Washington, London: Plenum Press)
- [2] Conyers and Herring 1937 *Phys. Rev.* **52** 361
- [3] Wigner E P 1959 *Group Theory and its Application to the Quantum, Mechanics of Atomic Spectra* (New York, London: Academic Press)
- [4] Thoma K, Dorner B, Duesing G and Wegener W 1974 *Solid State Commun.* **15** 1111
- [5] Hewat A W 1974 *Solid State Commun.* **8** 187
- [6] Schiff L I 1968 *Quantum Mechanics* (New York: McGraw-Hill)
- [7] Normand J-M A 1947 *Lie Group: Rotation in Quantum Mechanics* (North Holland Publishing Company)
- [8] Frobenius and Schur 1906 *Berl. Ber.* 186
- [9] Bir G L and Picus G E 1974 *Symmetry and Strain Induced Effects in Semiconductors* (John Wiley & Sons)
- [10] Kunert H W 1982 *Physica* **114** A 600-603
- [11] Kunert H W 2004 *Eur. Phys. J. Appl. Phys.* **27** 252
- [12] Kunert H W 2003 *Applied Surface Science* **212-213** 890
- [13] Lambrecht W R L and Segall B 1994 *Properties of Group III Nitrides* ed Edgar J H (London: INSPEC)
- [14] Lambrecht W R L, Segall B, Rife J, Hunter W R and Wickenden D K 1995 *Phys. Rev. B* **51** 13516
- [15] Rashba E I 1959 *Fiz. Tverd. Tel.* **1** 407 (English transl.: 1959 *Soviet Phys. Solid State* **1** 368)
- [16] Lyle P, Hamilton D R and Choyke W J 1966 *Phys. Rev.* **143** 526